Intersubject consistent dynamic connectivity during natural vision revealed by functional MRI

Xin Di [1, 2], Bharat B Biswal [1, 2 *]

1. Department of Biomedical Engineering, New Jersey Institute of Technology, Newark, NJ, 07029, USA

2. School of Life Sciences and Technology, University of Electronic Science and Technology of China, Chengdu, China

* Corresponding author:

Bharat B. Biswal, PhD

607 Fenster Hall, University Height

Newark, NJ, 07102, USA

bbiswal@yahoo.com

Abstract

The functional communications between brain regions are thought to be dynamic. However, it is usually difficult to elucidate whether the observed dynamic connectivity is functionally meaningful or simply due to noise during unconstrained task conditions such as resting-state. During naturalistic conditions, such as watching a movie, it has been shown that brain activities in the same region, e.g. visual cortex, are consistent across subjects. Following similar logic, we proposed to study intersubject correlations of the time courses of dynamic connectivity during naturalistic conditions to extract functionally meaningful dynamic connectivity patterns. We analyzed a functional MRI (fMRI) dataset when the subjects watched a short animated movie. We calculated dynamic connectivity by using sliding window technique, and further quantified the intersubject correlations of the time courses of dynamic connectivity. Although the time courses of dynamic connectivity are thought to be noisier than the original signals, we found similar level of intersubject correlations of dynamic connectivity. Most importantly, highly consistent dynamic connectivity could occur between regions that did not show intersubject correlations of regional activity, and between regions with little stable functional connectivity. The analysis highlighted higher order brain regions such as the lateral prefrontal cortex and the default mode network that dynamically interact with posterior visual regions during the movie watching, which may be associated with the understanding of the movie.

Keywords: default mode network; dynamic connectivity; intersubject correlation; naturalistic condition; supramarginal gyrus

Highlights

- Intersubject shared time courses may provide a complementary approach to study dynamic connectivity
- Widespread regions showed highly shared dynamic connectivity during movie watching, while these regions themselves did not show shared regional activity
- Shared dynamic connectivity often occurred between regions from different functional systems

1. Introduction

The functional communications between spatially remote brain regions, especially the dynamics of connectivity, is a key to understand brain functions (Bullmore and Sporns, 2012; Friston, 2011; Park and Friston, 2013). Recently, the study of dynamic connectivity has drawn increasing research interest, especially in resting-state (Allen et al., 2014; Fu et al., 2019, 2018; Hutchison et al., 2013). However, due to the unconstrained nature of resting-state, it is difficult to elucidate whether the observed changes of connectivity across sliding windows are due to real fluctuations of functional communications, or simply due to random fluctuations (Lindquist et al., 2014). Moreover, the blood-oxygen-level dependent (BOLD) signals measured by fMRI are sensitive to physiological noises, such as respiration, heartbeat (Teichert et al., 2010), and head motion (Power et al., 2012), which may give rise to spurious correlation estimates for short window.

One way to capture meaningful dynamic functional connectivity is to manipulate subjects' mental states during the course of scan, so that there is known reference for the changes of connectivity. For example, in a typical task-based fMRI study with blocked design, different task conditions are assigned as blocks. Therefore, the time courses of dynamic connectivity can be correlated with the task design to identify task related connectivity changes (Di et al., 2015; Rosenthal et al., 2017). An alternative approach is to expose the subjects with naturalistic stimuli, such as a short movie. Although there is no predefined references of dynamic connectivity changes, one may take advantage of the phenomenon of intersubject correlation to capture changes that are consistent across different subjects (Hasson et al., 2004; Nastase et al., 2019).

In the seminal study, Hasson and colleagues calculated intersubject correlations of the time series of BOLD signal (Figure 1A) when the subjects were watching a movie (Hasson et al., 2004). They demonstrated that several brain regions, especially the visual cortex, are highly correlated across subjects during movie watching. We propose that similar approach can be applied to the time courses of dynamic connectivity to capture meaningful functional communication dynamics during natural vision. Specifically, dynamic connectivity is usually calculated using a sliding window approach, so that a time

series of dynamic connectivity can be obtained. The time courses of dynamic connectivity can then be correlated across-subjects (Figure 1B). If the dynamic connectivity reflects real time functional communications between regions that are caused by the viewing of natural stimuli, then the time courses of dynamic connectivity from different subjects should somehow correlated. Therefore, we can apply intersubject correlation method to identify meaningful dynamic communications between regions.

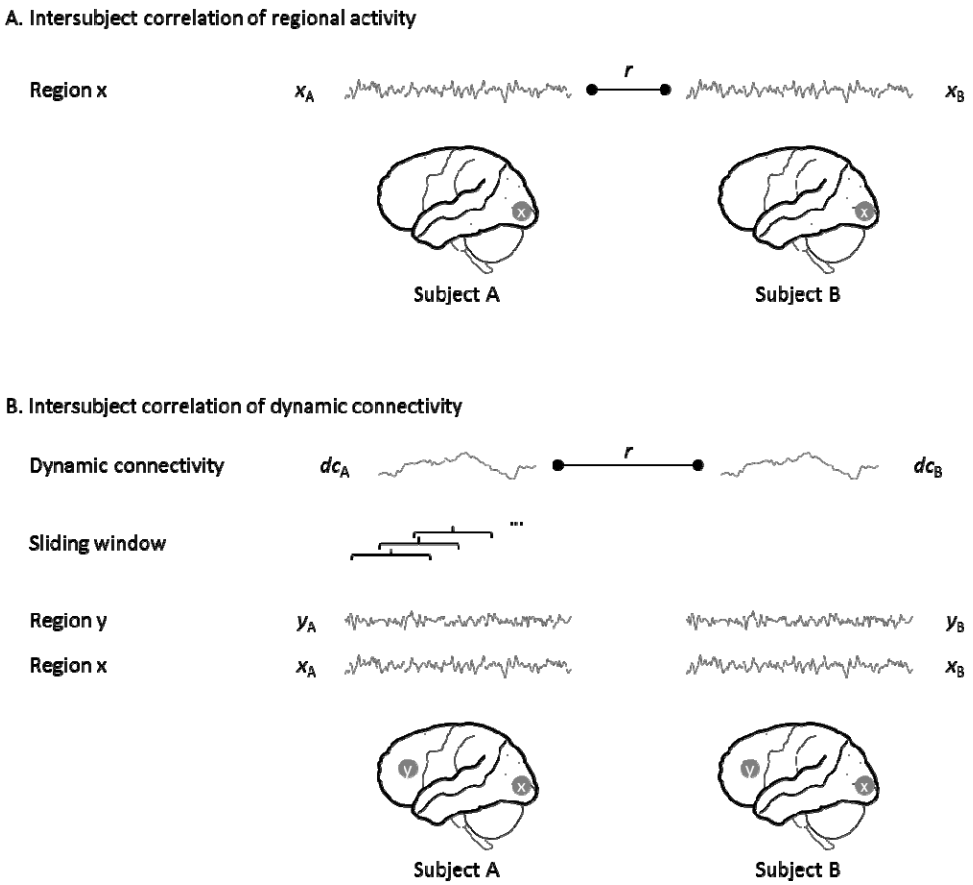

Figure 1 Illustrations of the calculations of intersubject correlations of the time series of regional activity (A) and the time courses of dynamic connectivity between two regions (B).

In the current study, we analyzed an fMRI dataset where the subjects were scanned when viewing a short animated movie. The aim was to identify dynamic connectivity that were shared cross subjects during the movie watching. In order to do so, we first performed regular intersubject correlation analysis to identify brain regions that showed consistent regional activity. Given these regions, we adopted a seed-

based strategy to calculate dynamic connectivity between a seed region and every voxels in the brain. We then evaluated and identified regions whose connectivity with the seed were consistent cross subjects. Even though higher order association regions did not typically show high intersubject correlations of regional activity (Hasson et al., 2004), their functional communications with lower order regions may be consistent across subject following the narrative of the movie. We therefore hypothesized that intersubject correlations of dynamic connectivity may be able to identify more widespread regions and functional dynamics that are associated with the watching of the movie.

2. Materials and methods

2.1. Data and task

The fMRI data were obtained through openneuro (https://openneuro.org/; accession #: ds000228). Only the data from adult subjects were analyzed. There were originally 33 adult subjects. Two subjects' data were discarded because of poor brain coverage (subject #: sub-pixar123 and sub-pixar123), and two were discarded due to large head motions (sub-pixar149 and sub-pixar150). As a result, a total of 29 subjects were included for the current analysis (17 females). The mean age is 24.6 years old (18 to 39 years).

During the fMRI scan, the subjects watched a silent version of Pixar animated movie "Partly Cloudy", which is 5.6 minutes long (https://www.pixar.com/partly-cloudy#partly-cloudy-1). Brain MRI images were acquired on a 3-Tesla Siemens Tim Trio scanner using the standard Siemens 32-channel head coil. Functional images were collected with a gradient-echo EPI sequence sensitive to BOLD contrast in 32 interleaved near-axial slices (EPI factor: 64; TR: 2 s, TE: 30 ms, flip angle: 90°). The voxel size were 3.13 mm isotropic, with 3 subjects with no slice gap and 26 subjects with 10% slice gap. 168 functional images were acquired for each subject, with four dummy scans collected before the real scans to allow for steady-state magnetization. T1-weighted structural images were collected in 176 interleaved sagittal slices with 1 mm isotropic voxels (GRAPPA parallel imaging, acceleration factor of 3; FOV: 256 mm). For more information for the dataset please refers to (Richardson et al., 2018).

2.2. FMRI data analysis

2.2.1. Preprocessing

FMRI data processing and analyses were performed using SPM12 and MATLAB (R2017b) scripts. A subject's T1 weighted structural image was first segmented into gray matter, white matter, cerebrospinal fluid, and other tissue types, and was normalized into standard Montreal Neurological Institute (MNI) space. The T1 images were then skull stripped based on the segmentation results. Next, all the functional images of a subject were realigned to the first image of the session and coregistered to the skull stripped T1 image of the same subject. Framewise displacement was calculated for the translation and rotation directions for each subject (Di and Biswal, 2015). Subjects who had maximum framewise displacement greater than 1.5 mm or 1.5^{o} were discarded from further analysis. The functional images were then normalized to MNI space using the parameters obtained from the segmentation step with resampled voxel size of 3 x 3 x 3 mm^3. The functional images were then spatially smoothed using a Gaussian kernel of 8 mm. Lastly, a voxel-wise general linear model (GLM) was built for each subject to model head motion effects (Friston's 24-parameter model) (Friston et al., 1996), low frequency drift (1/128 Hz), and constant offset. The residuals of the GLM were saved as a 4-D image series, which were used for further intersubject correlation analysis.

2.2.2. Intersubject correlation analysis

The correlations of time series of either brain activity or dynamic connectivity are calculated between pairs of subjects. If there are N subjects, then there will be N x (N-1) / 2 correlation coefficients. The statistics of these correlations become tricky, because they are calculated from only N subjects, therefore not independent. An alternative approach is leave-one-out (Nastase et al., 2019), where the time series of one hold-out subject were correlated with the averaged time series of the remaining N – 1 subjects. The averaged time series of N – 1 subjects were thought to reflect the consistent component rather than the noisy individual's time series. Therefore, the resulting correlations should be higher than the pair-wise correlations. Another benefit is that this approach estimates one correlation for each subject, making group level statistics easier. Therefore, we adopt the leave-one-out approach in the current analysis.

We first performed intersubject correlation analysis on regional activity time series. The preprocessed BOLD time series were extracted for each voxel and subject in a gray matter mask. For a given voxel, the time series of one subject was hold out, and the averaged time series of the remaining subject were calculated. Then the time series of the hold-out subject were correlated with the averaged time series. This process was performed for every subject and every voxel, resulting in one correlation map for one subject. The correlation maps were transformed into Fisher's z maps. Group level one sample t test was then performed to identify regions whose intersubject correlations were consistently greater than 0. However, the null hypothesis statistical significance testing may not provide much information of the effect size. There may be only small but consistent correlations for each subject, which could give rise to very high statistical significance in a one sample t test. Indeed, when doing such null hypothesis statistical significance testing for intersubject correlation analysis, usually almost all the brain regions will show somehow significant correlations (Chen et al., 2016). We are more interested and focused on the real effect size, i.e. correlation coefficients, in our analysis. We therefore averaged the Fisher's z maps, and transformed them back into r maps. The continuous r maps were shown in the results section.

We next performed intersubject correlation analysis on dynamic connectivity using a seed-based approach. Given that a set of brain regions showed high intersubject correlations of regional activity, we defined these regions as seeds. We adopted a relatively high threshold of $r > 0.45$ for the averaged intersubject correlation map of regional activity to isolate four visual related seeds. Two of the seeds were located in the medial and posterior portion of the occipital lobe, which mainly covered the lingual gyrus and calcarine sulcus. The other two seeds were located bilaterally in the middle occipital gyrus and extended to the middle temporal gyrus. We labeled them as left and right medial visual and lateral visual seeds, respectively. In addition, we adopted a relatively low threshold of $r > 0.35$ to isolate the left and right supramarginal gyrus seeds. For each seed, we performed a voxel-wise correlation analysis, i.e. calculating intersubject correlations of dynamic connectivity between the seed and every voxel in the gray matter mask. For two given time series from a seed and a voxel, we used sliding window technique to

calculate dynamic connectivity. The window length was set as 30 time points (60 s) (Nastase et al., 2019), and the time step was set as 2 time point (4 s). Therefore, the time course of dynamic connectivity had 70 window steps. Similarly, we calculated correlations between the time courses of dynamic connectivity of a given subject with the averaged dynamic connectivity of remaining subjects for a given voxel. As a result, there was one correlation map for each seed and subject.

The r maps of correlations of dynamic connectivity were transformed into Fisher's z maps for group level statistical analysis. Again, we also simply calculated averaged z map for a seed, and transformed it back into r map. In addition, we performed a voxel-wise repeated measure one way analysis of variance (ANOVA) to identify regions that showed specific dynamic connectivity patterns with different seeds.

In addition to the voxel-based analysis, we also performed region of interest (ROI)-based analysis for in-depth examinations of the dynamic connectivity effects. In addition to the six seeds, we included four more regions that showed high intersubject correlations of dynamic connectivity with the seeds. They were left precentral gyrus and left inferior frontal gyrus, which showed high intersubject correlations of dynamic connectivity with the medial visual seeds, and posterior cingulate cortex and medial prefrontal cortex, which showed high intersubject correlations of dynamic connectivity with the supramarginal gyrus seeds. The calculations of intersubject correlations of dynamic connectivity were the same as the seed-based analysis.

The selections of sliding window length is nontrivial (Fu et al., 2014; Zhang et al., 2013). In addition to the 30-TR window length, we also explored other window length of 10 TRs (20 s), 20 TRs (40 s), and 40 TRs (80 s). For each window length, we calculated intersubject correlations of dynamic connectivity among the 10 ROIs.

2.2.3. Stable functional connectivity

We also calculated stable functional connectivity among the 10 ROIs to compare them with the dynamic connectivity. First, for each subject, we calculated correlation coefficients across the 10 ROIs, and transformed them into Fisher's z. Then the z matrices were averaged across the 29 subjects, and

transformed back into r values. Second, we calculated the consistent component of each ROI, i.e. averaging the time series across the 29 subjects. And then one single correlation matrix among the 10 ROIs was calculated. This connectivity of the consistent component is essentially the same as intersubject functional connectivity proposed by Simony and colleagues (Simony et al., 2016).

3. Results

3.1. Intersubject correlations of regional activity

We first calculated intersubject correlations of regional activity for every voxel in the brain during the video watching (Figure 2A). The highest correlations were around 0.5. The major regions that had high intersubject correlations were the visual cortex extending anterior to the fusiform gyrus and middle temporal lobe. The bilateral supramarginal gyrus also showed high intersubject correlations. The bilateral precentral gyrus also showed intersubject correlations, but the effect sizes were much smaller. Figure 2A shows all the voxels with positive correlation values. It is noteworthy that many regions showed very small intersubject correlations, including largely the prefrontal cortex and anterior temporal lobe.

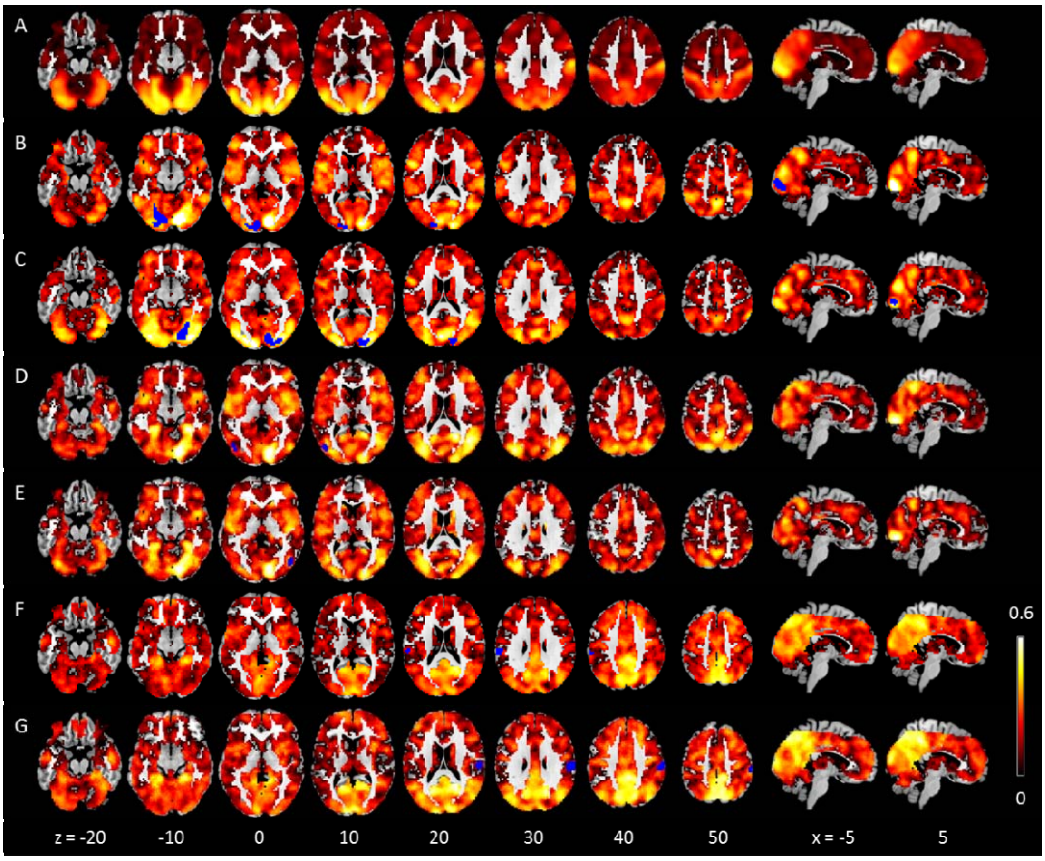

Figure 2 Intersubject correlation maps of regional activity (A) and dynamic connectivity with different seeds (B through G). The seed regions were depicted in blue in respective rows. All voxels with positive correlations are shown. The numbers at the bottom represent z and x coordinates in Montreal Neurological Institute (MNI) space.

3.2. Intersubject correlations of dynamic connectivity

3.2.1 Seed-based analysis

We defined seed regions where there were high intersubject correlations of regional activity, which included bilateral medical visual regions, lateral visual regions, and supramarginal gyrus. We next calculated voxel-wise intersubject correlations of dynamic connectivity with the six seeds, respectively (Figure 2B through 2G). There were widespread brain regions that showed intersubject consistent dynamic correlations with different seeds. First of all, the effect sizes of the intersubject correlations of

dynamic connectivity, i.e. the correlation coefficients, were comparable to those in the intersubject correlations of regional activity. Secondly, regions with intersubject correlations of dynamic connectivity turned out to be more widespread and extended to the frontal and temporal regions that did not show high intersubject correlations of regional activity. Thirdly, the left and right corresponding seeds showed similar dynamic connectivity patterns, but there are substantial different patterns of dynamic connectivity among medial visual, lateral visual, and supramarginal gyrus seeds. In order to highlight specific brain regions that showed dynamic connectivity with different seeds, we performed repeated measure ANOVA and compared the maps of different level of seeds with other seeds (Figure 3 and Table 1). The medical visual seeds showed consistent dynamic connectivity with mainly lateral brain regions, including the left inferior frontal gyrus/precentral gyrus, bilateral supramarginal gyrus, and left orbital gyrus/inferior frontal gyrus. The lateral visual seeds showed consistent dynamic connectivity with several visual regions. In contrast, the supramarginal seeds showed consistent dynamic connectivity with the precuneus/posterior cingulate gyrus, medial prefrontal cortex, and bilateral angular gyrus, which basically formed the default mode network.

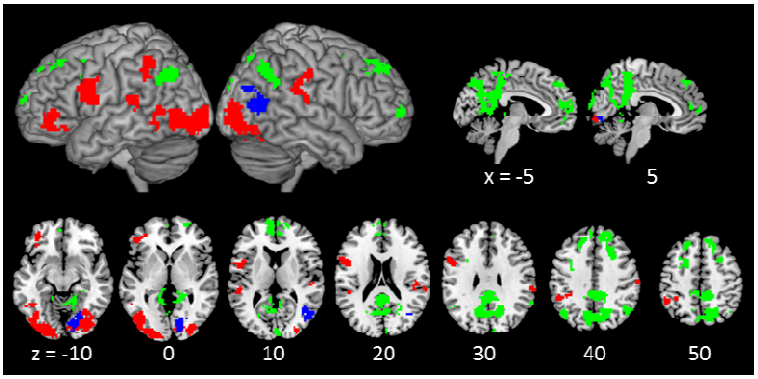

Figure 3 Differential intersubject correlations of dynamic connectivity among the medial visual, lateral visual, and supramarginal gyrus seeds. Red, medial visual seeds greater than lateral visual and supramarginal gyrus seeds. Blue, lateral visual seeds greater than medial visual and supramarginal gyrus seeds. Green, supramarginal gyrus seeds greater than medial and lateral visual seeds. All maps were thresholded at $p < 0.001$, and cluster thresholded at $p < 0.0167$ (0.05 / 3) after false discovery rate (FDR) correction.

3.2.2. Relationships with stable functional connectivity

In order to better understand and interpret the brain regions and connectivity relationships, we further calculated different types of connectivity measures among a set of regions of interest. In addition to the six seeds, we defined left precentral gyrus and left inferior frontal gyrus ROIs that showed higher dynamic connectivity with the medial visual seeds, and posterior cingulate cortex and medial prefrontal cortex ROIs that showed high dynamic connectivity with the supramarginal seeds. Among the 10 regions, we calculated regular mean functional connectivity (Figure 4A) and connectivity derived from the consistent components (Figure 4B). These two correlations matrices look similar, and clearly showed three clusters of brain regions. The first four regions were all visual. The fifth to eight regions were the bilateral supramarginal gyrus, and lateralized frontal regions, which were all high order association brain regions. The last two regions were part of the default mode network, which also showed negative correlations with the association regions in the consistent component correlations.

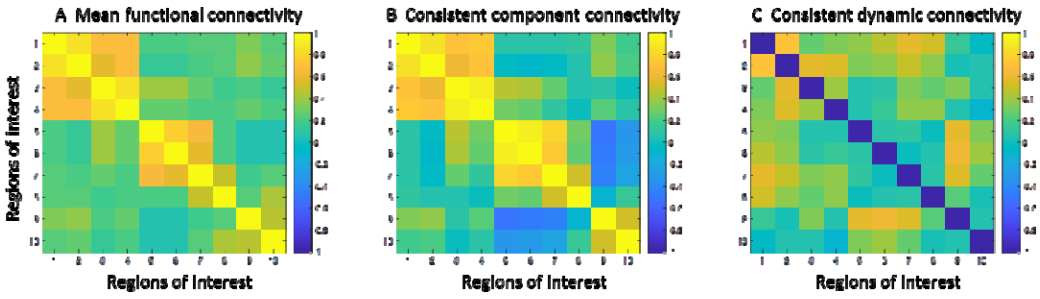

Figure 4 Correlation matrices among the 10 regions of interest (ROI) using different methods. A) Mean functional connectivity across the 29 subjects. B) Correlations of the consistent component of each ROI (averaged time series across the 29 subjects). C) Intersubject correlations of dynamic connectivity.

The intersubject consistent dynamic connectivity matrix (Figure 4C) was largely different from the two stable correlation matrices. Some high consistent dynamic connectivity was observed within the visual regions. The highest correlation was observed between the left and right medial visual regions (r = *0.70*). In contrast, many consistent dynamic connectivity were shown between different functional

networks, where there were virtually none or even negative stable correlations. Specifically, the medial visual regions showed high consistent dynamic connectivity with the left frontal regions. The highest intersubject correlation was 0.56 between left medial visual region and left precentral gyrus. The default mode regions and supramarginal regions also showed high consistent dynamic connectivity. The highest correlation was 0.60 between the posterior cingulate cortex and right supramarginal gyrus. It is noteworthy that these regions generally showed negative stable correlations in Figure 4B.

3.2.3. The time courses of dynamic connectivity

Lastly, we analyzed the time courses of dynamic connectivity for the above mentioned pairs of regions (Figure 5). The consistent dynamic connectivity between left and right medial visual regions was in general high, which is consistent with the results of stable connectivity. But it can be seen that the connectivity level went down during the first half of windows, and continued with two cycles of up and down fluctuations. The fluctuations rather than a monotonic linear trend suggest that the dynamics of connectivity is not simply due to sensory habituations. The left medial visual region and left precentral gyrus did not show high level of correlations in general. But it had small positive correlations at the beginning of the run, went down to around zero, and then went back to small positive correlations. What is more interesting is the dynamic connectivity between the right supramarginal gyrus and posterior cingulate cortex, where the connectivity switched between positive and negative values during the whole course.

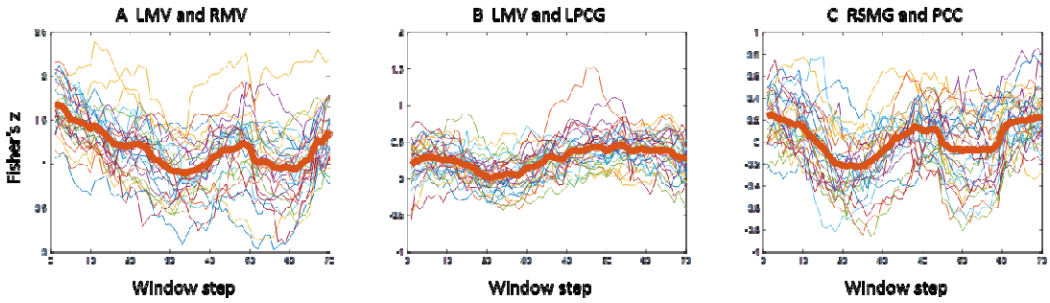

Figure 5 Time courses of dynamic connectivity (Fisher's z) for three pairs of brain regions. Each thinner line represents the time course of one subject, and the thicker red lines represent the averaged time

courses. LMV, left medial visual; RMV, right medial visual; LPCG, left precentral gyrus; RSMG, right supramarginal gyrus; PCC, posterior cingulate cortex.

3.2.4. The effects of sliding-window length

We repeated the ROI-based intersubject correlation analysis of dynamic connectivity using different window length from 10 TRs to 40 TRs. The overall patterns of intersubject correlations of dynamic connectivity looked similar (Figure 6), especially for the 30-TR window and 40-TR window results. But the correlation values were weaker for shorter window lengths, especially for 10-TR window length. The bottom row of Figure 6 illustrated the time courses of dynamic connectivity of a typical pair of regions, i.e. the right supramarginal gyrus and posterior cingulate cortex. It can be seen that for short window, e.g. 10-TR window, the time course of dynamic connectivity were very noisy. Moreover, the fluctuations of dynamic connectivity changed fast, and it seems that different subjects had different delays of certain increases or decreases of connectivity. For longer window, the dynamic connectivity time courses became smoother, and the fluactuations across subjects were more aligned across subjects, which in turn gave rise to higher intersubject correlations.

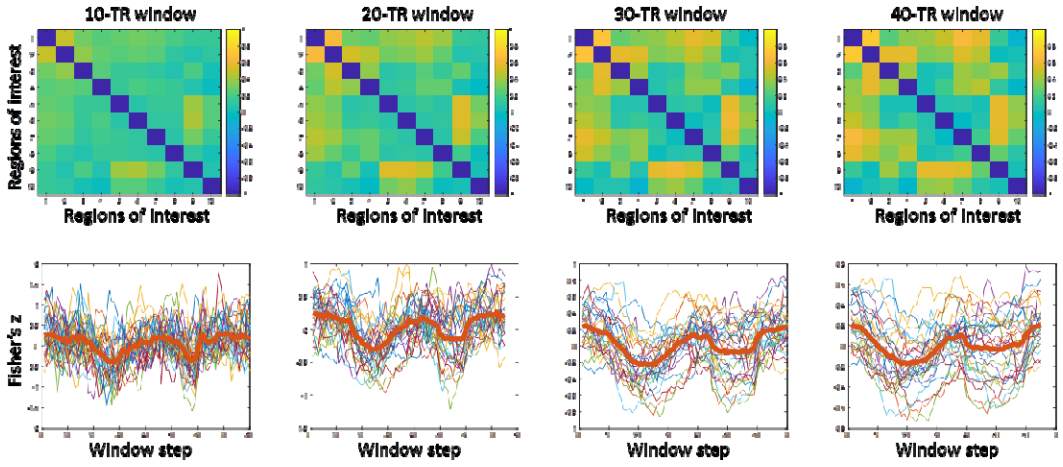

Figure 6 The effects of sliding-window length on the intersubject correlations of dynamic connectivity (top row), and on the time courses of dynamic connectivity between the right supramarginal gyrus and posterior cingulate cortex (bottom row).

4. Discussion

In the current study, we proposed intersubject correlation analysis on the time courses of dynamic connectivity during natural vision. We were able to identify intersubject consistent dynamic connectivity at similar level as the intersubject correlations of regional activity, although the time courses of dynamic connectivity were thought to be nosier than the original time series. By using seed regions from the visual cortex and supramarginal gyrus, we demonstrated widespread brain regions that showed high intersubject consistent dynamic connectivity with these seeds, although these regions themselves did not show intersubject correlations of regional activity. These regions included high order association regions such as the left precentral cortex and left inferior frontal gyrus, as well as the default mode network. The intersubject consistent patterns of dynamic connectivity support the functional meaningfulness of dynamic connectivity during movie watching, and suggest that dynamic connectivity could be a complementary avenue to characterize the functions of a brain region.

The brain regions that had the highest intersubject correlations of regional activity are mainly in the posterior visual related regions, which are consistent with previous studies (Hasson et al., 2004; Nummenmaa et al., 2012). In addition to this, the current study also found high intersubject correlations among different levels of visual areas, and the highest intersubject correlation of dynamic connectivity was between the left and right medial visual regions. This is interesting because the dynamic connectivity is on top of overall high level of stable functional connectivity (Figure 4A). The observable dynamics of connectivity among visual areas are also consistent with previous studies showing task modulated connectivity among visual areas in different task conditions (Di et al., 2018, 2015; Di and Biswal, 2017).

In addition to the dynamic connectivity among visual regions, the visual regions also showed consistent dynamic connectivity with regions outside the visual network. Specifically, the medial visual regions showed high intersubject correlations of dynamic connectivity with the bilateral supramarginal gyrus, left precentral gyrus, and left inferior frontal gyrus, which are all high order association areas. The

stable connectivity results also showed that there were high stable connectivity among these association regions, but weak stable connectivity with the visual regions, further confirmed that they were two functional modules in the brain. In addition, the supramarginal gyrus, which is a part of the task positive network (Fox et al., 2005), showed high intersubject correlations with the default mode network. The stable connectivity results also showed negative correlations between the supramarginal gyrus and default mode network regions, which further confirmed they were from two different functional modules. These results suggest that the functional communications between the regions from different functional modulates are not stable, but highly depend on task contexts (Bullmore and Sporns, 2012). It is also consistent with findings that the connectivity between regions from different functional modules are more dynamic and context dependent (Di and Biswal, 2019; Fu et al., 2017).

The supramarginal gyrus is the major region outside the visual cortex that showed high intersubject correlations of regional activity. The involvements of supramarginal gyrus of intersubject correlations are inconsistent in the literature (Hasson et al., 2004; Kauppi et al., 2010), which probably due to different movies used. Given its critical role in empathy (Silani et al., 2013), it is reasonable to find high intersubject correlations in the supramarginal gyrus during the watching of the animated movie, which involves the understanding the intentions of different animated characters. More interestingly, we also found that the default mode network showed high intersubject correlations of dynamic connectivity with the supramarginal gyrus seeds. Similar to a previous study on the dynamics of intersubject connectivity (Simony et al., 2016), both of the studies highlighted the critical role of the default mode network in understanding of the narratives of a movie.

The selection of window length for dynamic connectivity analysis is nontrivial (Fu et al., 2014; Zhang et al., 2013). The shorter the window length, the finer the temporal resolution for dynamic connectivity could be. Nevertheless, there would also be less number of time points for each window, resulting in noisier estimates of connectivity. The current results showed that the overall patterns of intersubject correlation matrices of dynamic connectivity were similar across different window length. But the effect sizes changed dramatically. From Figure 6, it seems that in shorter window length, e.g. 10-

TR, the dynamic connectivity time courses were not only noisier, but also with intersubject variability of delays. The offset of connectivity fluactuations across subjects might compromise the intersubject correlations. But when longer window length was used, the time courses become smoother, therefore becoming more intersubject correlated. In other words, the consistent component of dynamic connectivity reflects a slow and averaged pattern of dynamic communication between brain regions. Further studies may use other correlations methods that were not sensitive to phase delays, e.g. coherence, to capture dynamic patterns of connectivity in a finer temporal scale.

5. Conclusion

In the current study, we proposed intersubject correlation analysis on dynamic connectivity. The results revealed widespread brain regions that showed consistent intersubject correlations of dynamic connectivity. The consistent correlations support the functional significance of dynamic connectivity during natural vision. The method may provide complementary approach to understand the dynamic nature of brain functional integrations.

Acknowledgement:

This study was supported by grants from (US) National Institute of Health (R01 AT009829; R01 DA038895).

Conflict of interest

The authors declared that there is no conflict of interest.

References:

Allen, E.A., Damaraju, E., Plis, S.M., Erhardt, E.B., Eichele, T., Calhoun, V.D., 2014. Tracking whole-brain connectivity dynamics in the resting state. Cereb. Cortex N. Y. N 1991 24, 663–76. https://doi.org/10.1093/cercor/bhs352

Bullmore, E., Sporns, O., 2012. The economy of brain network organization. Nat. Rev. Neurosci. 13, 336–349. https://doi.org/10.1038/nrn3214

Chen, G., Shin, Y.-W., Taylor, P.A., Glen, D.R., Reynolds, R.C., Israel, R.B., Cox, R.W., 2016. Untangling the relatedness among correlations, part I: Nonparametric approaches to inter-subject correlation analysis at the group level. NeuroImage 142, 248–259. https://doi.org/10.1016/j.neuroimage.2016.05.023

Di, X., Biswal, B.B., 2019. Toward Task Connectomics: Examining Whole-Brain Task Modulated Connectivity in Different Task Domains. Cereb. Cortex 29, 1572–1583. https://doi.org/10.1093/cercor/bhy055

Di, X., Biswal, B.B., 2017. Psychophysiological Interactions in a Visual Checkerboard Task: Reproducibility, Reliability, and the Effects of Deconvolution. Front Neurosci 1–36. https://doi.org/10.3389/fnins.2017.00573

Di, X., Biswal, B.B., 2015. Characterizations of resting-state modulatory interactions in the human brain. J. Neurophysiol. 114, 2785–96. https://doi.org/10.1152/jn.00893.2014

Di, X., Fu, Z., Chan, S.C., Hung, Y.S., Biswal, B.B., Zhang, Z., 2015. Task-related functional connectivity dynamics in a block-designed visual experiment. Front. Hum. Neurosci. 9, 1–11. https://doi.org/10.3389/fnhum.2015.00543

Di, X., Zhang, Z., Biswal, B.B., 2018. Psychophysiological interaction and beta series correlation for task modulated connectivity: modeling considerations and their relationships. bioRxiv 322073. https://doi.org/10.1101/322073

Fox, M.D., Snyder, A.Z., Vincent, J.L., Corbetta, M., Van Essen, D.C., Raichle, M.E., 2005. The human brain is intrinsically organized into dynamic, anticorrelated functional networks. Proc. Natl. Acad. Sci. U. S. A. 102, 9673–8.

Friston, K.J., 2011. Functional and effective connectivity: a review. Brain Connect. 1, 13–36. https://doi.org/10.1089/brain.2011.0008

Friston, K.J., Williams, S., Howard, R., Frackowiak, R.S., Turner, R., 1996. Movement-related effects in fMRI time-series. Magn. Reson. Med. Off. J. Soc. Magn. Reson. Med. Soc. Magn. Reson. Med. 35, 346–55. https://doi.org/DOI 10.1002/mrm.1910350312

Fu, Z., Chan, S.-C., Di, X., Biswal, B., Zhang, Z., 2014. Adaptive covariance estimation of non-stationary processes and its application to infer dynamic connectivity from fMRI. IEEE Trans. Biomed. Circuits Syst. 8, 228–39. https://doi.org/10.1109/TBCAS.2014.2306732

Fu, Z., Tu, Y., Di, X., Biswal, B.B., Calhoun, V.D., Zhang, Z., 2017. Associations between Functional Connectivity Dynamics and BOLD Dynamics Are Heterogeneous Across Brain Networks. Front. Hum. Neurosci. 11. https://doi.org/10.3389/fnhum.2017.00593

Fu, Z., Tu, Y., Di, X., Du, Y., Pearlson, G.D., Turner, J.A., Biswal, B.B., Zhang, Z., Calhoun, V.D., 2018. Characterizing dynamic amplitude of low-frequency fluctuation and its relationship with dynamic functional connectivity: An application to schizophrenia. NeuroImage 180, 619–631. https://doi.org/10.1016/j.neuroimage.2017.09.035

Fu, Z., Tu, Y., Di, X., Du, Y., Sui, J., Biswal, B.B., Zhang, Z., de Lacy, N., Calhoun, V.D., 2019. Transient increased thalamic-sensory connectivity and decreased whole-brain dynamism in autism. NeuroImage 190, 191–204. https://doi.org/10.1016/j.neuroimage.2018.06.003

Hasson, U., Nir, Y., Levy, I., Fuhrmann, G., Malach, R., 2004. Intersubject synchronization of cortical activity during natural vision. Science 303, 1634–40. https://doi.org/10.1126/science.1089506

Hutchison, R.M., Womelsdorf, T., Allen, E. a., Bandettini, P. a., Calhoun, V.D., Corbetta, M., Della Penna, S., Duyn, J.H., Glover, G.H., Gonzalez-Castillo, J., Handwerker, D. a., Keilholz, S., Kiviniemi, V., Leopold, D. a., de Pasquale, F., Sporns, O., Walter, M., Chang, C., 2013. Dynamic functional connectivity: Promise, issues, and interpretations. NeuroImage 80, 360–378. https://doi.org/10.1016/j.neuroimage.2013.05.079

Kauppi, J.-P., Jääskeläinen, I.P., Sams, M., Tohka, J., 2010. Inter-subject correlation of brain hemodynamic responses during watching a movie: localization in space and frequency. Front. Neuroinformatics 4. https://doi.org/10.3389/fninf.2010.00005

Lindquist, M.A., Xu, Y., Nebel, M.B., Caffo, B.S., 2014. Evaluating dynamic bivariate correlations in resting-state fMRI: A comparison study and a new approach. NeuroImage 101, 531–546. https://doi.org/10.1016/j.neuroimage.2014.06.052

Nastase, S.A., Gazzola, V., Hasson, U., Keysers, C., 2019. Measuring shared responses across subjects using intersubject correlation. Soc. Cogn. Affect. Neurosci. 14, 667–685. https://doi.org/10.1093/scan/nsz037

Nummenmaa, L., Glerean, E., Viinikainen, M., Jääskeläinen, I.P., Hari, R., Sams, M., 2012. Emotions promote social interaction by synchronizing brain activity across individuals. Proc. Natl. Acad. Sci. U. S. A. 109, 9599–9604. https://doi.org/10.1073/pnas.1206095109

Park, H.-J., Friston, K., 2013. Structural and Functional Brain Networks: From Connections to Cognition. Science 342, 1238411–1238411. https://doi.org/10.1126/science.1238411

Power, J.D., Barnes, K.A., Snyder, A.Z., Schlaggar, B.L., Petersen, S.E., 2012. Spurious but systematic correlations in functional connectivity MRI networks arise from subject motion. NeuroImage 59, 2142–2154. https://doi.org/10.1016/j.neuroimage.2011.10.018

Richardson, H., Lisandrelli, G., Riobueno-Naylor, A., Saxe, R., 2018. Development of the social brain from age three to twelve years. Nat. Commun. 9, 1–12. https://doi.org/10.1038/s41467-018-03399-2

Rosenthal, G., Sporns, O., Avidan, G., 2017. Stimulus Dependent Dynamic Reorganization of the Human Face Processing Network. Cereb. Cortex 27, 4823–4834. https://doi.org/10.1093/cercor/bhw279

Silani, G., Lamm, C., Ruff, C.C., Singer, T., 2013. Right Supramarginal Gyrus Is Crucial to Overcome Emotional Egocentricity Bias in Social Judgments. J. Neurosci. 33, 15466–15476. https://doi.org/10.1523/JNEUROSCI.1488-13.2013

Simony, E., Honey, C.J., Chen, J., Lositsky, O., Yeshurun, Y., Wiesel, A., Hasson, U., 2016. Dynamic reconfiguration of the default mode network during narrative comprehension. Nat. Commun. 7, 12141. https://doi.org/10.1038/ncomms12141

Teichert, T., Grinband, J., Hirsch, J., Ferrera, V.P., 2010. Effects of heartbeat and respiration on macaque fMRI: Implications for functional connectivity. Neuropsychologia 48, 1886–1894. https://doi.org/10.1016/j.neuropsychologia.2009.11.026

Zhang, Z.G., Fu, Z.N., Chan, S.C., Hung, Y.S., Motta, G., Di, X., Biswal, B.B., 2013. Adaptive window selection in estimating dynamic functional connectivity of resting-state fMRI, in: 2013 9th International Conference on Information, Communications & Signal Processing. IEEE, pp. 1–4. https://doi.org/10.1109/ICICS.2013.6782935

Table 1 Clusters with differential intersubject correlations of dynamic connectivity among the medial visual, lateral visual, and supramarginal gyrus seeds. All clusters were thresholded at $p < 0.001$, and cluster thresholded at $p < 0.0167$ (0.05 / 3) after false discovery rate (FDR) correction.

		MNI Coordinates				
cluster FDR	Voxel	x	y	z	Peak t	Label
Medial visual > (lateral visual + supramarginal)						
< 0.001	157	-51	8	23	6.00	Left precentral gyrus
< 0.001	439	-12	-100	-4	5.90	Occipital pole
< 0.001	87	-51	-49	50	5.23	Left supramarginal gyrus
< 0.001	86	-33	44	-10	5.15	Left lateral orbital gyrus
< 0.001	408	24	-88	-4	5.10	Right inferior occipital gyrus
0.007	46	-60	-58	5	5.05	Left middle temporal gyrus
< 0.001	95	66	-31	26	4.92	Right supramarginal gyrus
0.003	57	-48	-34	14	4.58	Left planum temporale
Lateral visual > (medial visual + supramarginal)						
< 0.001	165	15	-79	-4	6.09	Lingual gyrus
< 0.001	99	48	-70	8	5.98	Right inferior occipital gyrus
Supramarginal > (medial visual + lateral visual)						
< 0.001	1582	6	-40	44	6.92	Precuneus
< 0.001	142	-3	59	8	5.87	Medial superior frontal gyrus
< 0.001	254	27	11	47	5.50	Right middle frontal gyrus
< 0.001	105	-30	11	35	5.38	Left middle frontal gyrus
0.001	77	-45	-67	38	5.17	Left angular gyrus
< 0.001	90	48	-61	44	4.98	Right angular gyrus
< 0.001	85	-21	29	50	4.83	Left superior frontal gyrus
< 0.001	104	24	62	2	4.79	Right superior frontal gyrus
0.006	49	0	-91	11	4.40	Cuneus

MNI, Montreal Neurological Institute